

# Mapping dynamical systems onto complex networks

E.P. Borges<sup>1,a</sup>, D.O. Cajueiro<sup>2,b</sup>, and R.F.S. Andrade<sup>3,c</sup>

<sup>1</sup> Escola Politécnica, Universidade Federal da Bahia, 40210-630 Salvador, Brazil

<sup>2</sup> Departamento de Economia, Universidade Católica de Brasília, 70790-160 Brasília, Brazil

<sup>3</sup> Instituto de Física, Universidade Federal da Bahia, 40210-340 Salvador, Brazil

Received 30 October 2006 / Received in final form 30 July 2007

Published online 22 September 2007 – © EDP Sciences, Società Italiana di Fisica, Springer-Verlag 2007

**Abstract.** The objective of this study is to design a procedure to characterize chaotic dynamical systems, in which they are mapped onto a complex network. The nodes represent the regions of space visited by the system, while the edges represent the transitions between these regions. Parameters developed to quantify the properties of complex networks, including those related to higher order neighbourhoods, are used in the analysis. The methodology is tested on the logistic map, focusing on the onset of chaos and chaotic regimes. The corresponding networks were found to have distinct features that are associated with the particular type of dynamics that generated them.

**PACS.** 89.75.Fb Structures and organization in complex systems – 89.75.Hc Networks and genealogical trees – 02.10.Ox Combinatorics; graph theory

## 1 Introduction

Chaotic dynamical systems are characterized by several measures that quantify how irregular, albeit deterministic, the trajectories are. The set of Lyapunov exponents [1] provides a measure of the dependence of the trajectories of the dynamical systems on the initial conditions, while information theory may be used to characterize such systems in terms of the production of entropy. In fact, a dynamical system with chaotic behaviour may be regarded as an example of Shannon's concept of an ergodic information source [2], since the Kolmogorov-Sinai entropy is equal [3] to the sum of the positive Lyapunov exponents. Further measures used to describe a chaotic system include fractal dimensions and singularity spectra [4, 5]. This formalism applies only when the system has at least one positive Lyapunov exponent. However, several authors have studied the particular situation of the quadratic logistic map when its Lyapunov exponent vanishes [6–9]. In this case, the distance between trajectories that are very close at  $t = 0$  fluctuates over time. Depending on the value of  $t$ , the distance either increases or decreases, since the envelope of the fluctuations of this distance is composed of two branches, one increasing and the other decreasing as power laws [7–9]. This particular situation may be considered typical of other systems with a larger number of equations in which the largest Lyapunov exponent vanishes. These situations are usually found at the onset of

chaos, when an infinitesimal change of a control parameter drives the system into either a regular or a chaotic regime. These investigations revealed some of the features regarding the sensitivity to the initial conditions [6], entropy production per unit time [10], multifractal geometry of the attractor [11], relaxation to the system attractor [12] and multifractal dynamics at the onset of chaos [13].

Recently, the investigation of complex networks has set up a new framework for the analysis of systems with many degrees of freedom. Within this framework, access is obtained to the properties of the topological structure underlying the mutual interactions among the components of the system. This approach has been applied to a large variety of actual systems, ranging from social interactions, biological data, internet and electrical power distribution [14, 15].

This paper defines a procedure to map a dynamical system onto a network. The network properties can then be used to display new features to characterize the trajectory of the system. The network nodes correspond to coarse-grained regions (cells) of the phase space visited by the trajectory. Two nodes  $r$  and  $s$  are linked when, during the time evolution, the trajectory jumps from cell  $r$  to cell  $s$ . Although this naturally offers a construction procedure for a directed network, in this paper only undirected networks are considered. In this approach, novel geometric and topological properties of the phase space are evaluated through the measures that have been recently developed to characterize complex networks. The dynamical system defined on the time domain is mapped onto a node domain, which represents the regions of the

---

<sup>a</sup> e-mail: [ernesto@ufba.br](mailto:ernesto@ufba.br)

<sup>b</sup> e-mail: [danoc@pos.ucb.br](mailto:danoc@pos.ucb.br)

<sup>c</sup> e-mail: [randrade@ufba.br](mailto:randrade@ufba.br)

phase space visited by the trajectory. As it is based on the division of phase space into boxes, this process follows construction procedures similar to those considered in the evaluation of the fractal dimension of attractors and the Kolmogorov-Sinai entropy.

It should be mentioned that some previous studies have already tried to combine some ideas of dynamical systems and complex networks. As this paper shows, however, our approach is rather different, as the previous contributions consider synchronization under the assumption of a certain regularity in the connection topology [16,17]. The use of a network to represent the phase space evolution of discrete time dynamical systems has also been suggested [18].

In this report, we restrict to the analysis of the quadratic map [19] described by

$$x_{t+1} = 1 - ax_t^2 \quad (t = 0, 1, 2, 3, \dots) \quad (1)$$

where  $x_t \in [-1, 1]$  and  $a \in [0, 2]$ . Equation (1) leads to a variety of distinct dynamical situations, the properties of which are expected to be manifested in the networks from which they originate. In particular, three regimes are investigated: the onset of chaos, which proceeds through a bifurcation cascade; the immediate neighbourhood of an intermittency transition; and the fully developed chaos.

## 2 Network characterization

An undirected network  $R$  is defined only by the number of nodes ( $N$ ) and links ( $L$ ), represented by an assembly of unordered pairs  $S_R(r, s)$ ,  $r, s \leq N$ , indicating which pairs of nodes are directly connected. This information provides a full description of the network, leading to computation of the average number of links per node  $\langle k \rangle$ , the average clustering coefficient  $C$ , the mean minimal distance among the nodes  $\langle d \rangle$ , the diameter  $D$ , and the probability distribution  $p(k)$  of nodes with  $k$  links. Other measures, such as the assortativity degree [20] and the distribution of clustering coefficients  $C(k)$  of individual nodes with respect to their degree  $k$ , have also been introduced, but they will not be discussed in this paper.

$R$  may be described in terms of its adjacency matrix  $M(R)$ . This is not the most concise representation of a network, but it opens the possibility of evaluating its spectral properties and, as recently indicated, the higher order neighbourhoods  $R_\ell$ ,  $\ell = 1, 2, \dots, D$  [21]. This is done in a straightforward way, by means of the set of matrices  $\{M_\ell\}$ , so defined that  $(M_\ell)_{r,s} = 1$  only if the shortest distance along the network between the nodes  $r$  and  $s$  is  $\ell$ . Otherwise,  $(M_\ell)_{r,s} = 0$ . Although all the information on the network is contained in  $S_R(r, s)$  or in  $M(R)$ , each  $M_\ell$  condenses information on  $R$  that is extracted from  $M(R)$  within the quoted framework. This formalism is also consistent with the recently proposed procedure to evaluate the fractal dimension of the network  $d_{F,R}$  [22], as it naturally leads to the set  $\{N_\ell\}$  required for this evaluation. Here, each  $N_\ell$  counts the number of pairs of nodes that are  $\ell$  steps apart.

Within this framework, each node is considered the only zeroth order neighbour of itself, and we express this by defining  $M_0 = I$ , where  $I$  indicates the identity matrix. In addition, it is assumed that  $M_1 = M$ . Since the only possible values of the matrix elements of  $M(R)$  are 0 or 1, the other matrices  $M_\ell$  of the set are recursively evaluated using Boolean operations [21]. Further use will be made of a matrix that condenses all information in  $\{M_\ell(R)\}$ . As previously discussed, given any two nodes  $r$  and  $s$ , it is clear that  $(M_\ell)_{r,s} = 1$  for just one value of  $\ell$ . Therefore, if we define a matrix

$$\widehat{M} = \sum_{j=0}^{\ell_{max}} j M_j, \quad (2)$$

it will provide direct information on the number of steps between any two nodes in the network. Furthermore, this information in  $\widehat{M}$  may be used to graphically illustrate the structure of a network with the use of colour or gray scale plots.

It should also be mentioned that this framework opens the door to a more precise characterization of the network, if we consider each  $R_\ell$  as an independent network. Therefore, several of the aforementioned properties used to characterize  $R$  may also be used for the evaluation of  $R_\ell$ . This is discussed in the next section, specifically with respect to the degree distribution and clustering coefficient  $\langle k \rangle_\ell$  and  $C(\ell)$ .

## 3 An algorithm to map a dynamical system onto a network

In order to map a dynamical system onto a network  $R$ , we use the framework of an algorithm introduced some time ago [23], which was originally conceived to efficiently evaluate the generalized fractal dimensions of fractal structures by the box counting method.

With respect to a dynamical system with  $m$  variables one may consider, without loss of generality, a set of points  $\mathcal{Z} \subset \mathbb{R}^m$  consisting of the vectors  $z(i)$ ,  $i = 1, \dots, T$ ,  $T \gg 1$ , which represent the coordinates of the dynamical system. The components of these vectors,  $z_\delta(i)$ ,  $\delta = 1, \dots, m$ , are assumed to belong to the interval  $[0, 1)$ . A graining in phase space is defined by dividing each phase space axis into  $W$  equally sized disjoint intervals, so that the whole phase is spanned by a set of  $W^m$  boxes. This also represents the maximum possible number of nodes in a network, for example, in the case of an ergodic system. Of course, the choice of  $W$  defines the graining, and the size of the region represented by a node. In the next section the effect of  $W$  on the obtained networks is evaluated.

Based on [23], each point  $z(i)$  of the trajectory is mapped onto a node of  $R$  according to

$$n(i) = \sum_{\delta=1}^m W^{\delta-1} \text{floor}(W z_\delta(i)), \quad (3)$$

where  $\text{floor}(x)$  is a function that evaluates the largest integer less than  $x$ . In fact, this is merely a simple way of dividing the region  $[0, 1]^m$  into equal parts. The nodes of the network thus constructed represent a box in the coarse-grained phase space of the system. After the mapping is complete, the boxes that were not visited by the trajectory are eliminated from the network, as they constitute nodes with zero degree ( $k = 0$ ), which do not provide any useful information on the dynamical system. The edges are built as described in the following procedure. Suppose that  $z(i)$  and  $z(i + 1)$  be two consecutive points of the dynamical system, and that these points were previously mapped onto the nodes  $n(r)$  and  $n(s)$ , where  $0 < r, s \leq W^m$ . Then, one introduces an edge connecting  $n(r)$  and  $n(s)$ . Here, it is considered that there is only one edge linking  $n(r)$  to  $n(s)$  and that self-links are not allowed.

This procedure may lead to directed and weighted networks; however, this paper focuses on the simplest situation of undirected and unweighted networks, since our main purpose is to address the problem and show that useful information may be extracted from it.

## 4 Results

This study concentrated on values of  $a$  in three different regions,  $a = a_c = 1.40115518909\dots$ ,  $a \in [1.749, 1.75)$  and  $a = 2$ , which correspond, respectively, to the first period doubling transition, the region close to the tangent bifurcation to the period-three window, and the fully developed chaotic state.

Representative networks for the different chaotic attractors are generated for different values of the graining  $W$ . Only trajectories that start on the attractor were considered in order to avoid spurious nodes (those visited only once) that depend on initial conditions. For a fixed value  $W$ , the network grows as the trajectory evolves in the phase space with respect to the number of iteration steps  $t$ . There is no a priori criterion to decide the time  $t_F$  after which the network is complete. In this study, we followed the way in which  $N$  and  $L$  increase with respect to  $t$ , for a given  $W$ .  $t_F$  is defined as the smallest value of  $t$  for which  $N(t_F) = N(2t_F)$  and  $L(t_F) = L(2t_F)$ .

First let us discuss the effect of  $W$  on  $N$  and  $L$ . To present a full neighbourhood analysis of the networks, we have selected here values of  $W$  that lead to the maximal number  $\approx 10\,000$  nodes in the network. The choice of  $W$  clearly depends on  $a$ . Indeed, due to the strategy adopted for the construction of the networks,  $N$  grows with  $W$  according to a power law mediated by the fractal dimension of the attractor  $d_{F,A}$ . This is shown in Figure 1a, in which points are drawn, in logarithmic scale, for  $a = a_c$ ,  $a_c + 10^{-3}$ , 1.749999 and 2. For  $a_c$ , the slope is  $0.54\dots$ , which agrees with the known value of  $d_{F,A}$  of the period doubling attractor. In all other cases, the slope is 1 within an accuracy of 2%, even for  $a = a_c + 10^{-3}$ , which lies already in the chaotic regime. This is in accordance with the fact that  $d_{F,A}$  changes in a discontinuous way at  $a = a_c$ . When  $a$  corresponds to a periodic solution, the network

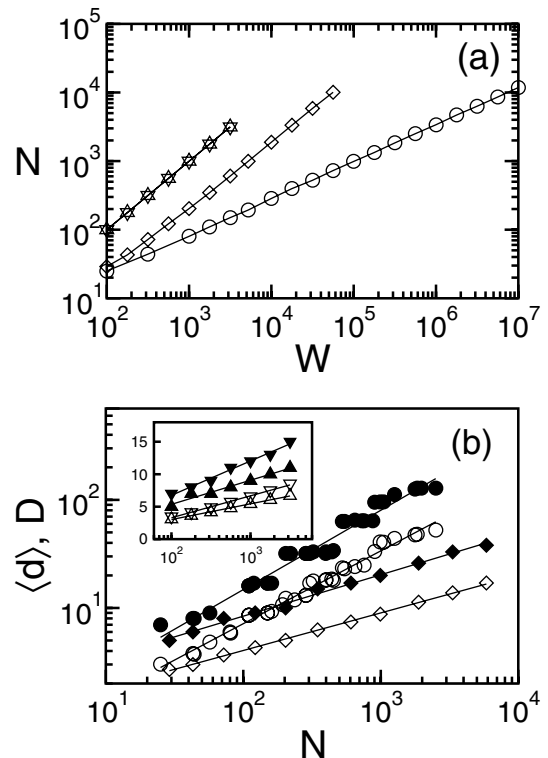


**Fig. 1.** (a) Dependence of  $N$  with respect to  $W$  for  $a = a_c$  (circles),  $a = a_c + 10^{-3}$  (diamonds),  $a = 1.749999$  (down triangles), and  $a = 2$  (up triangles). The same convention is used in all other figures. The different slopes indicate the values of  $d_{F,A}$ . (b) Power law dependence of  $\langle d \rangle$  (hollow symbols) and  $D$  (solid symbols) with respect to  $N$  for  $a = a_c$  and  $a = a_c + 10^{-3}$ . The inset shows logarithmic dependence among the same quantities when  $a = 1.749999$  and  $a = 2$ .

becomes finite, so that  $N$  and  $L$  do not depend on  $W$ , provided this parameter is large enough.

Although we are primarily interested in the properties of the complete network, it is also possible to follow the dependency of  $N$  and  $L$  with respect to  $t$ , for a fixed value of  $W$ . Assuming  $N \sim L^z$ , this defines a dynamical exponent  $z$  in the early stages of evolution of the network. The analyzed data indicate that  $z \simeq 1$  for all values of  $a$ . Nevertheless, in the immediate chaotic neighbourhood of  $a = 1.75$ , the laminar phases in the intermittent regime are found to trap the trajectory for long intervals, demanding a large time of integration to complete the network.

The network properties will now be discussed in accordance with the aforementioned methodology and parameters. Whenever appropriate, this discussion is extended to include properties of higher order neighbourhoods in the network. Different network structures are found if we consider the chaotic regime or the onset of chaos. With respect to the mean minimal distance  $\langle d \rangle$  and diameter  $D$ , in the case of the chaotic regime, these are found to grow with respect to  $W$  (and  $N$ ), in a logarithmic way, similar to that of small-world networks [24]. If  $\langle d \rangle = \alpha \log_{10} W$ , then  $\alpha \simeq 2.4$  and  $3.7$ , respectively, for  $a = 2$  and  $a \in [1.749, 1.749999]$ , as illustrated in the inset

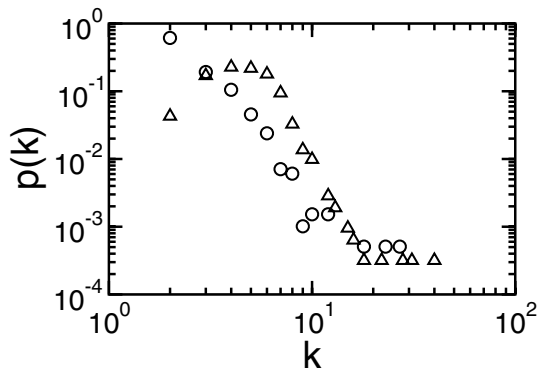


**Fig. 2.** Degree distribution of nodes at  $a_c$  (circles) and in the  $a = 2$  chaotic regime, (up triangles). Behaviour close to tangent bifurcation,  $a = 1.75 \cdot 10^{-4}$ , (not shown) is quite similar to  $a = 2$ .

of Figure 1b. As  $D$  only assumes integer values, a similar power law pattern, that would be expected, appears only in an approximate way, with equally sized steps in  $D \times \log_{10} W$  plots. Therefore, assuming  $D = \beta \log_{10} W$ , the result is  $\beta \simeq 4$  for  $a = 2$  with a very high level of accuracy. In the interval  $[1.749, 1.749999]$ , we noticed the presence of fluctuations in the size of the steps, which increases when we approach the threshold  $a = 1.75$ . The results for  $a = a_c$  behave completely differently:  $\langle d \rangle$  and  $D$  increase as power laws with respect to  $W$ , as illustrated in the main panel of Figure 1b. For  $a = a_c + 10^{-3}$ , the same type of dependence prevails. The exponents obtained for  $\langle d \rangle$  and  $D$  are, respectively, 0.67 and 0.73 for  $a_c$ , and 0.35 and 0.38 for  $a = a_c + 10^{-3}$ .  $\langle d \rangle$  and  $D$  increase smoothly for  $a = a_c + 10^{-3}$ . However, at  $a = a_c$ , discontinuities and steps appear in the plots of these parameters. The results shown in Figure 1b indicate that, unlike the properties of the attractor, reflected by the sudden change in the value of  $d_{F,A}$ , the network properties change slowly when the chaotic regime is reached.

The distribution  $p(k)$  vs.  $k$  was evaluated in each one of the different regimes. In the case of  $a = a_c$ , as shown in Figure 2,  $k$  does not reach large values ( $k_{max} \simeq 30$ ). Therefore, it is not possible to identify a power law decay in this range. For  $a = 2$  (and also  $a = 1.749999$ ) nodes with larger values of  $k$  may be found, but  $p(k)$  does not follow a power law either.

This distinctive behaviour is also present when we analyze the fractal dimension of the network  $d_{F,R}$  [22]. Figure 3 shows that the  $a = a_c$  networks have a well defined scaling behaviour, which extends extremely precisely over more than two decades. On the other hand, there is no evidence of a fractal dimension for the networks in the chaotic regime. First, the small values of  $D$  reduces the region of possible scaling behaviour. In addition, deviations to the expected power-law regime can be clearly observed.

With respect to the clustering coefficient, we obtain  $C \equiv 0$  when  $a = a_c$ , indicating the complete absence of triangles in the network. In the case of  $a = 1.749999$  or  $a = 2$ ,  $C$  is small and decays with  $N$  according to a power law with exponent  $\approx 0.95$ , what is far from the

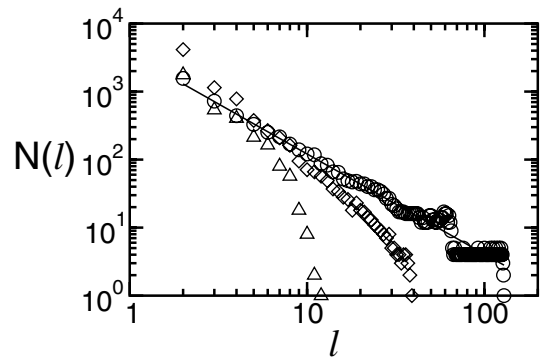


**Fig. 3.** Clear power law behaviour for  $N(\ell) \times \ell$  when  $a = a_c$ , with  $d_{F,R} = 1.47$ . Finite size effects blur this dependence when  $\ell \simeq D$ . In the chaotic regime, for  $a = 2$ ,  $d_{F,R}$  can not be evaluated. For  $a = a_c + 10^{-3}$ , the points illustrate a slow transition between the two regimes.

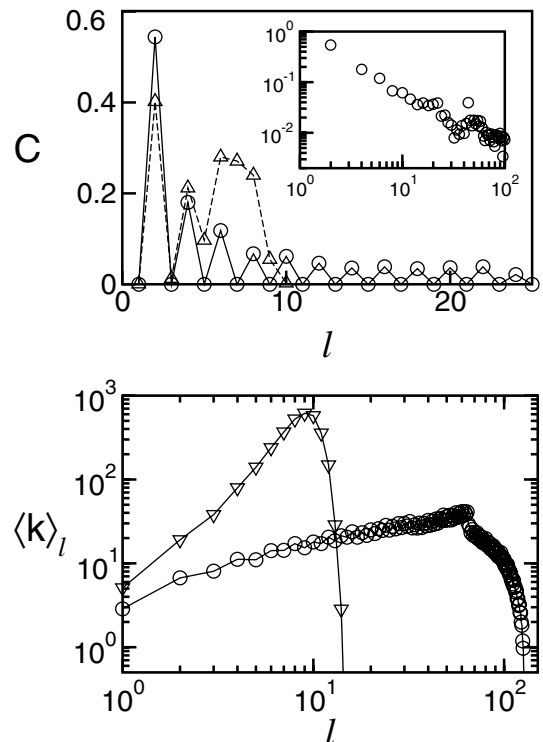


**Fig. 4.** (a) Behaviour of  $C(\ell)$  with respect to  $\ell$  for chaotic regime and at the onset of chaos. The inset shows a peculiar power law behaviour  $C(\ell)$  at the onset of chaos. (b) Behaviour of  $\langle k \rangle_\ell \times \ell$ . The onset of chaos shows a slowly increasing value of  $\langle k \rangle_\ell$  over a large interval of  $\ell$ , interrupted by finite size effects already present in Figure 3. In contrast with this picture, the chaotic regime shows a sharp increase in  $\langle k \rangle_\ell$ .

value of 0.75 observed for the Albert-Barabasi scale-free network [14]. However, these small values indicate that the network has only a small number of triangles.

Other features of the network may be drawn if we consider the clustering coefficient of higher order neighbourhoods [21]. To obtain a clearer picture of this analysis consider, for instance, the regular Cayley tree where each



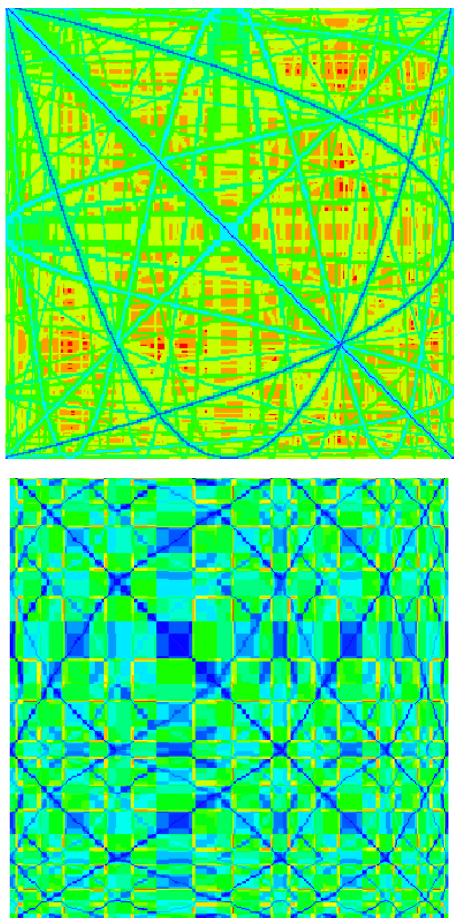


**Fig. 5.** Colour scale plots (gray scale in the paper version) of  $\widehat{M}$  for  $a = 2$  (a) and  $a = a_c$  (b). Scale ranges from black and blue ( $\ell = 0$  and  $\ell = 1$ ) to red ( $\ell = D$ ). Number of levels in (a) is much smaller than in (b). Neighbourhood structure changes abruptly in the distinct regimes.

site has coordination 3. The  $\ell = 2$  network is formed by triangles, in much the same way as the Husimi cactuses, resulting in a correspondingly large value for  $C(\ell = 2)$ . The following odd and even numbered neighbourhoods are characterized, respectively, by values of  $C(\ell) = 0$  and  $C(\ell) > 0$ , whereby the values of  $C(\ell)$  for a subset of even neighbourhoods decrease monotonically. A similar situation is found with respect to the networks investigated here. In Figure 4a the sequence of  $C(\ell)$  is summarized for the three situations under investigation. For  $a = 2$  and  $a = 1.4999$ , the oscillatory behaviour was found to last only until  $\ell = 5$  and 10, respectively. In addition, the odd numbered  $C(\ell)$  was found to increase until reaching values as high as those of the even numbered neighbourhoods. On the other hand, the  $a = a_c$  network has  $C(\ell) = 0$  for all odd numbered neighbourhoods. The inset shows that the  $C(\ell = \text{even number})$  decays with  $\ell$  according to a power law, with exponent  $\alpha \simeq 1$ .

The average degree  $\langle k \rangle_\ell$  was also analyzed as a function of the neighbourhood  $\ell$ . Here again, the behaviour of the chaotic regime and the onset of chaos were found to have distinct features, as shown in Figure 4b.

Finally, the information in  $\widehat{M}$  was used to obtain in colour or gray scale images of the network neighbourhood structure. These images provide clear, simple visualization of their distinct properties of the attractor. For  $a = 2$ , the first order neighbourhood is distributed along the parabola described by the r.h.s. of (1) (see Fig. 5a). This illustrates how the second and higher order neighbourhood evolve according to the higher order iterates of the quadratic map. However, mixing and finite size effects stemming from a finite graining blurs the higher order iterates. The situation is different in the case of  $a_c$ , when the attractor is a  $d_{F,A} = 0.54\dots$  dust spread out in the  $[-1, 1]$  interval. Only boxes containing part of the dust remain in the network, so that contiguous numbered nodes are not actually neighbours in phase space. The resulting image (Fig. 5b) displays a fine, intertwined tessitura that reflects a very peculiar behaviour of the trajectories at the onset of chaos [7–9].

## 5 Conclusion

In this paper, the idea of mapping chaotic systems onto complex networks is explored. Networks are constructed according to a well defined methodology, and results using the logistic map indicate how their properties are associated with those of the attractor in phase space. Trajectories in distinct dynamical regimes are investigated in order to show how the major differences in phase space are reflected in the networks. The networks show several features of small-world and scale-free networks, but these features do not completely match those generated by the specific algorithms described in [24,25]. The analysis of the networks in the neighbourhood of  $a_c$  reveals that the  $N \times W$  dependence, measured by  $d_{F,A}$ , undergoes sharp transition at the onset of chaos. Therefore, the distinct character of the trajectories in phase space is indeed reflected in the network. However, with the exception of  $C$ , the results for the other indices ( $\langle d \rangle$ ,  $D$  and  $p(k)$ ) change in a much smoother way with respect to changes in the parameter  $a$ .

This work was supported by the Brazilian Agencies CNPq and FAPESB.

## References

1. J.P. Eckmann, D. Ruelle, *Rev. Mod. Phys.* **57**, 617 (1985)
2. R.G. Gallager, *Information theory and reliable communication* (Addison-Wesley, Reading, MA, 1968)
3. Y.B. Pesin, *Rus. Math. Surv.* **32**, 55 (1977)
4. H.G.E. Hentschel, I. Procaccia, *Physica D* **8**, 435 (1983)
5. C. Meneveau, K.R. Sreenivasan, *Phys. Lett. A* **137**, 103 (1989)
6. C. Tsallis, A.R. Plastino, W.M. Zheng, *Chaos Solitons and Fractals* **8**, 885 (1997)
7. F. Baldovin, A. Robledo, *Phys. Rev. E* **69**, 045202 (2004)
8. A. Robledo, *Europhys. News* **36**, 214 (2005)
9. H. Hernández-Sandaña, A. Robledo, *Physica A* **370**, 286 (2006)

10. V. Latora, M. Baranger, A. Rapisarda, C. Tsallis, Phys. Lett. A **273**, 97 (2000)
11. M.L. Lyra, C. Tsallis, Phys. Rev. Lett. **80**, 53 (1998)
12. E.P. Borges, C. Tsallis, G.F.J. Añãños, P.M.C. de Oliveira, Phys. Rev. Lett. **89**, 254103 (2002)
13. E. Mayoral, A. Robledo, Phys. Rev. E **72**, 026209 (2005)
14. R. Albert, A.-L. Barabasi, Rev. Mod. Phys. **74**, 47 (2002)
15. S. Boccaletti, V. Latora, Y. Moreno, M. Chavez, D.U. Hwang, Phys. Rep. **424**, 175 (2006)
16. A. Pikovsky, M. Rosenblum, J. Kurths, *Synchronization - a universal concept in nonlinear science* (Cambridge University Press, Cambridge, 2001)
17. F.M. Atay, J. Jost, Phys. Rev. Lett. **92**, 144101 (2004)
18. S. Thurner, Europhys. News **36**, 218 (2005)
19. P. Collet, J.P. Eckman, *Iterated Maps on the Interval as Dynamical Systems* (Birkhauser, Boston, 1980)
20. M.E.J. Newman, Phys. Rev. Lett. **89**, 208701 (2002)
21. R.F.S. Andrade, J.G.V. Miranda, T.P. Lobão, Phys. Rev. E **73**, 046101 (2006)
22. C.M. Song, S. Havlin, H.A. Makse, Nature **433**, 392 (2005)
23. A. Block, W. VonBloh, H.J. Schellnhuber, Phys. Rev. A **42**, 1869 (1990)
24. D.J. Watts, S.H. Strogatz, Nature **393**, 440 (1998)
25. A.-L. Barabasi, R. Albert, Science **286**, 509 (1999)